Influence of process parameters on the formability of bead stamping part using advanced models

To cite this article: W Cha *et al* 2017 *J. Phys.: Conf. Ser.* **896** 012005

View the article online for updates and enhancements.

Related content

Influence of process parameters on the formability of bead stamping part using advanced models

W Cha[1]**, S Müller**[2]**, N Bursac**[2]**, A Albers**[2]** and W Volk**[1]

[1] Institute of Metal Forming and Casting, Technical University of Munich
Walther-Meissner-Str. 4, 85748, Garching, Germany

[2] Institute of Product Engineering, Karlsruhe Institute of Technology
Kaiserstr. 10, 76131, Karlsruhe, Germany

E-mail: wan-gi.cha@utg.de

Abstract. Beads are applied to deep drawn sheet metal parts to increase its stiffness. In order to form the bead, a two-stage manufacturing process including at least deep drawing and beading is performed. Thus, reductions of sheet metal thickness and consequently weight reduction can be effectively reached by numeric optimization. In order to apply the optimization algorithm to the production of non-virtual actual parts, the forming limits of the parts must be considered in both manufacturing steps. Bead formability is affected by process parameters such as blank holding force and lubrication. One way to investigate these influences is to use an accurate simulation model. In this study, the yield function named Yld2000-2D under non-associated flow rule is used to express anisotropic material behavior of blank and the Generalized Forming Limit Concept (GFLC) considering nonlinear strain paths is used to determine the formability. These models are validated by comparing the strain and bead forming limits measured in the Nakajima experiment. Then, the influences of mentioned process parameters are investigated by the validated model.

1. Introduction

The weight reduction of metal parts has recently been greatly required due to environmental and fuel efficiency savings. Even light products require high stiffness for safety. One way is to add bead geometry to deep drawn parts to increase the stiffness. The changed geometry through the bead can lead to more product stiffness than necessary. The weight of the part is reduced because the product thickness can be reduced by the margin of stiffness.

As the development of computer technology, numerical analysis technique was used to determine bead geometries that gives higher stiffness, and several numerical techniques and determination criteria have been proposed. Typically, the bead optimization includes a topological approach through material changes and a topographical approach suitable for positioning and orienting the bead. A beading optimization criteria by topographical approach was introduced that orientation of beads must be determined ideally along the trajectories of the first principal stress [1]. Recently, this algorithm have been developed in bead optimization [2]. The algorithms for the optimization of beads have not taken into manufacturing processes as well as the geometry of the sheet metal part.

Through this a bead optimization can be used for the development of new product generations based on reference products. In the case of product development projects, this can be sufficiently described by means of the PGE – Product Generation Engineering – approach [3].

In order to determine the ideal position of the bead, the load case and the stress distribution of the deformed part are required. For accurate formability, GFLC [4] which is a concept to predict the forming limit of metal sheet considering nonlinear strain path is used in this study. The GFLC requires major and minor strains as input. In the optimization process, the load cases are predetermined in consideration of the user, but the stress and strain distributions are provided in the forming process analysis. For this reason, the accuracy of the forming process analysis is a key factor in optimizing beading. The finite element method is used for the analysis of the forming process. Material models and variables have a great influence on the accuracy compared to other element sizes, numbers, and boundary conditions. The material parameters depend on the material model and anisotropic models are used to predict thin plate deformation. Among the anisotropic models, there is Hill48 [5], which express relatively simple expressions. These model has limitations that do not predict biaxial deformation and material behavior of aluminum well. Yld2000-2d [6] was proposed to express both directional r-values and yield stresses.

This study confirms the influence of the process parameters on the part formability after establishing the correct analysis model and the ideal beading location. The Yld2000-2D material model is used to calculate the stress and strain required for GFLC to be used for beading positioning and formability determination. After verification of the model, the effect of process parameters and formable parameter area are investigated using reliability analysis provided by LS-Opt [7], a program that automates many optimization algorithms.

2. PGE and optimization of bead location and orientation

Often development projects in the industry are based by the development of existing products (reference products), a so-called new product generation. In accordance with Albers et al. [3] starting from the reference products and their subsystems, three different components can be distinguished in the development of a new product generation. The adoption variation, which mainly involves adaptations of interfaces, the principle variation, in which the underlying principle is changed and the shape variation, in which only the shape is adapted [3]. In the case of a bead optimization the stiffness of the product is at the focus, thereby a variation in the shape of the reference product is necessary. The development of a new product generation on the basis of reference products allows the re-use of existing subsystems and available knowledge [3]. If the bead optimization is considered, the reference product without beads acts as input. With different load conditions and parameter of the bead in the optimization the best possible shape of the new product generation can be identified.

The basis of the bead optimization is the geometry as well as the load conditions of the component. The resulting main loads define position and course of trajectories. These are the basis for the location and orientation of the bead. Taking into account the optimum criterion, according to the orientation of the bead along the main bending stresses, the main bending paths are determined as primary trajectories. For this purpose, the main bending stress in 2D shell elements is calculated on the basis of a decomposition of the main stress state into the membrane stress component and the bending stress component. Starting points for the primary bending stress trajectories are the elements with the largest main bending stresses. These points are usually located inside the component, so the trajectory must be determined in both directions. A termination of the trajectory take place by the end of the component or due to other boundary conditions. Also, a design area in which the trajectory may only be allowed can be determined.

3. Simulation for pre- and bead forming

To form the bead, the first preforming and the second bead forming are performed. The Abacus program is used to simulate this process. Yld2000-2D is used to express the anisotropy of the sheet material. GFLC is selected in order to determine the formability of the material. Two algorithms are implemented

using VUMAT, which are user subroutine formats for Abaqus/explicit [8], and Excel, respectively. The strain results from Abaqus are exported and evaluated in GFLC written in Excel using the python program language. It also facilitates automated analysis through the LS-Opt optimization program. Description of each algorithm, model building and simple verification of it will be explained.

3.1. Generalized Forming Limit Concept (GFLC)

The GFLC have been firstly introduced by Volk et al. [4]. With this concept, it is possible to identify the beginning of local instability in two-stage forming processes. In case of two-step forming operations the traditional FLCs are not suitable to estimate the onset of necking. The GLFC using metamodeling allows the estimation of a localized instability for a given preforming condition. The dimensionless evaluated value λ indicates how close to the material instability is, and by normalization it can be shown to reach the forming limit of the material, when the value reaches 1.0 [9]. The reliability and detail of the GFLC was introduced in [4, 9].

3.2. Non-associated Yld2000-2D

The Yld2000-2D proposed by Barlat et al. [6] predict accurately yield stress and r-value directionalities covering rolling, diagonal, and transverse directions as well as balanced biaxial stress state. This model requires eight experimental results such as yield stress and r-value for rolling, transverse and diagonal directions and for balanced biaxial stress state ($r_0, r_{45}, r_{90}, r_b, \sigma_0, \sigma_{45}, \sigma_{90}, \sigma_b$) in order to determine the model parameters. The above model parameters are determined under the assumption of associate flow rule (AFR) that the yield function and the potential function are same, but more material variables are needed under the non-associate flow rule (non-AFR) that the yield function and the potential function do not coincide. The parameters of yield function are determined based on directional yield stress at every 15° from rolling direction and balanced biaxial stress ($\sigma_0, \sigma_{15}, \sigma_{30}, \sigma_{45}, \sigma_{60}, \sigma_{75}, \sigma_{90}, \sigma_b$). Furthermore, the parameters of the potential need the r-values from uniaxial tensile test in different orientations and balanced biaxial loading ($r_0, r_{15}, r_{30}, r_{45}, r_{60}, r_{75}, r_{90}, r_b$). Total 16 parameters are used for the non-AFR. This method was presented by [10]. Although more model parameters are needed, non-AFR can better represent r-values and stresses in different directions than AFR.

In order to determine the material characteristics, the uniaxial tensile and bulge test for HC260LAD and AA6016 with thickness of 1 mm are performed. The biaxial flow curves from the bulge test can be determined in higher strain range. The biaxial flow curves for HC260LAD and AA6016 are fitted to Swift [11] and combination of Swift and Hockett-Sherby [12] equation, respectively. The fitted equations are shown in equation (1) and (2).

$$\sigma_{HC260LAD} = 675.2(0.0051 + \varepsilon^p)^{0.199} \text{ MPa} \tag{1}$$

$$\sigma_{AA6016} = 0.1[412.8(0.0059 + \varepsilon^p)^{0.21}] + 0.9[369.5 - (369.6 - 146)\exp(-4.12\varepsilon^{p\,0.75})] \text{ MPa} \tag{2}$$

After that, the model parameters for AFR and non-AFR with Yld2000-2D are identified by using the calculation method of anisotropic coefficients introduced in [6] and [13], respectively. The AFR and non-AFR models are implemented as VUMAT in Abaqus [8]. In order to verify the model and parameters, uniaxial tensile test simulations were carried out at each 15° from rolling to transverse direction. One square element with a length of 1 mm was stretched to a displacement of 0.2 mm. The normalized stresses and r-values in each direction were evaluated at the equivalent plastic strain of 0.1. The values are compared with experimental values and shown in figure 1 and 2.

(a)   (b)
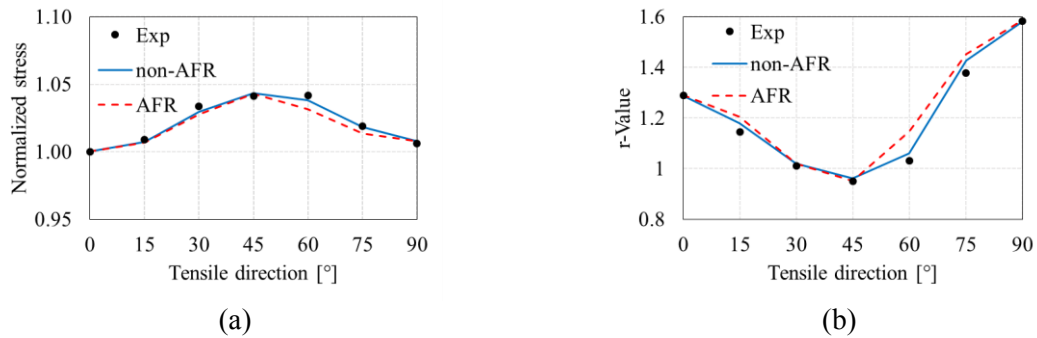
Figure 1. Comparison of directional normalized stresses (a) and Lankford coefficients (b) for HC260LAD

(a)   (b)
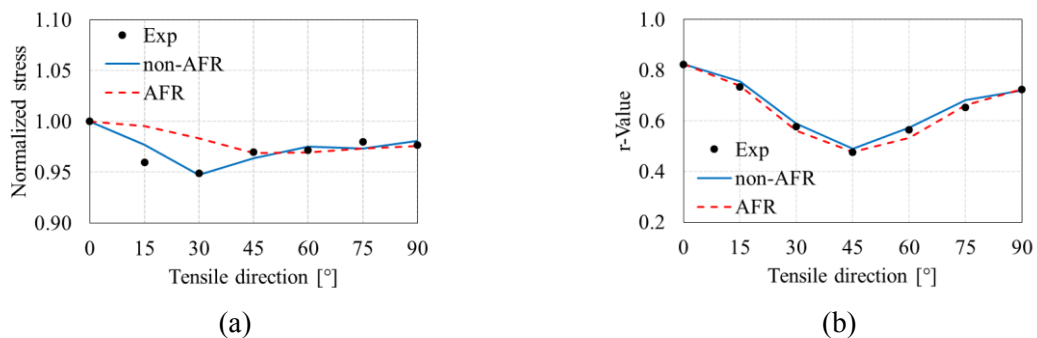
Figure 2. Comparison of directional normalized stresses (a) and Lankford coefficients (b) for AA6016

In the figure 1 (a), the normalized stress values in the AFR and non-AFR models are almost identical, but the non-AFR model is closer to the experimental values at 60° in the tensile direction. In figure 1(b), both models approximated the experimental values, but non-AFR predicts more accurately. The difference between the two models for the AA6016 is significant in the normalized stress comparison of figure 2 (a). Because the AA6016 material has high stress anisotropy, the non-AFR model approaches the experimental value more accurately than the AFR model at 15° and 30° in the tensile direction. On the other hand, it is shown that the calculated values of the two models are in agreement with the r-values in figure 2 (b). By using the non-AFR model with Yld2000-2D that can express more accurate material anisotropy, it is intend to obtain the accurate strain values required for the GFLC model used to predict the forming limit of the material. As the accuracy of the model was already confirmed, only non-AFR models are used thereafter.

(a)   (b)
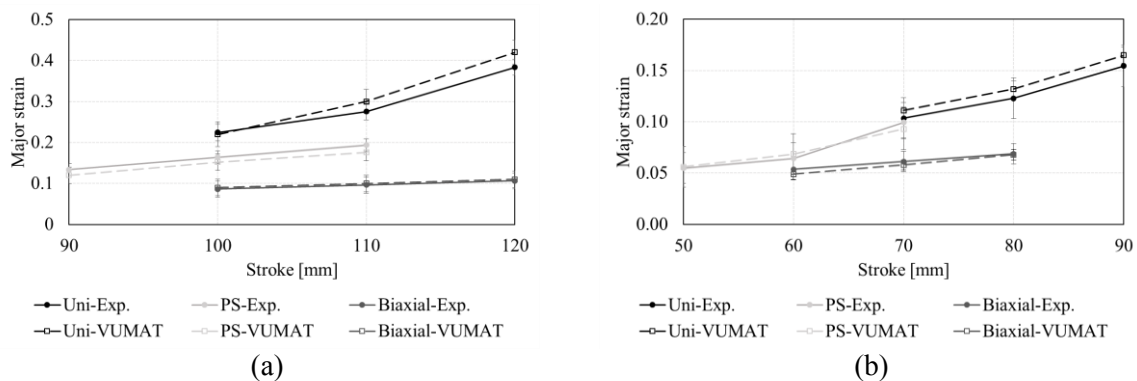
Figure 3. Comparison of major strains on apex of the sheet at the modified Nakajima test and simulation for HC260LAD (a) and for AA6016 (b)

3.3. Experimental validation

The modified Nakajima simulation with punch radius of 200 mm introduced in previous study [14] was performed in order to validate the implemented model. The major strains on the apex of sheet are evaluated. The sheet geometries have three different initial geometries to describe uniaxial, plain strain and biaxial forming. The comparison of major strains are shown in figure 3.

The simulation predicted the strain adequately for all cases in figure 3 (a) and (b). The simulation values are slightly higher for uniaxial tension for both materials. However, considering the minimum maximum error range, the deviation does not have a significant effect on the material formability prediction.

### 3.4. Finite element model for bead forming

The product by the modified Nakajima experiment has a hemispherical shape. For this geometrical reason, the product has high rigidity by preforming before bead forming. To confirm the higher stiffness effect by bead insertion, this study selects the tool geometries [15] for the preforming as shown in figure 4 and 5.
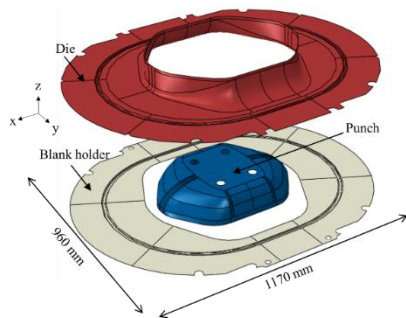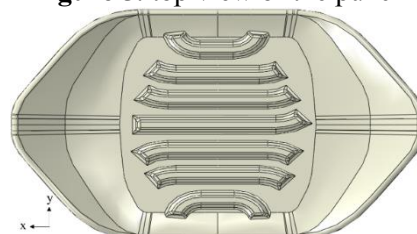

Figure 4. the tools for the preforming
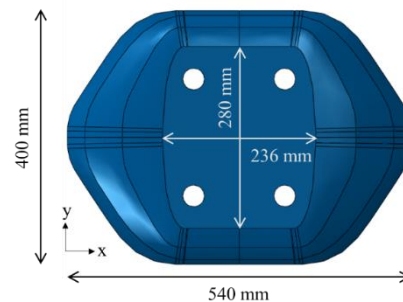
Figure 5. top view of the punch
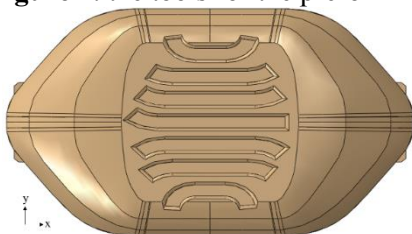
**Figure 6.** top view of the lower bead tool

Figure 7. top view of the upper bead tool

The punch tool named modified Marciniak [15] preformed the part of the sheet metal. The punch geometry has a plane with dimensions 236 mm x 280 mm. Due to the plane, the preformed parts can have lower stiffness, unlike the parts made by the Nakajima experiment. This makes it easier to confirm the effect of increasing the stiffness after the bead forming. If initial shapes of the specimen are different, parts with various strain states can also be formed by the modified Marciniak tool. In this study, only the biaxial specimen is used because it is important to identify the allowable process parameter space through the reliability analysis. The biaxial specimen has dimensions 920 mm x 1050 mm. After biaxial preforming, the bead forming is performed with the bead tools which are shown in figure 6 and 7. Figure 8 shows the selected loading case in this study. A rod with a 50 mm diameter circular cross section was pushed over the plane of the part to a z-axis displacement of 30 mm. The optimized bead position was determined for this load case. To account for the actual manufacturability of the ideal bead path mentioned above, beads are placed only in the part plane at a minimum gap of 40 mm between the bead paths. In this study, the cross section is constant along the path as it only changes the process parameters. The height of the cross section is 6 mm, the width is 30 mm, the edge radius is 5 mm, and the flank angle is 40 degrees. The definition of section was mentioned in [14].

3.5. Stiffening part by bead geometry

Figure 9 compares the stiffness of the part with the maximum load before and after the bead forming. Obviously, under the same load conditions, the maximum load required is further increased in the bead-formed part. For both materials HC260LAD and AA6016, the maximum load increased by about 30 %. The effect of increasing the stiffness by bead forming was confirmed. The next section examines which process parameters range this bead formed part can be actually produced.
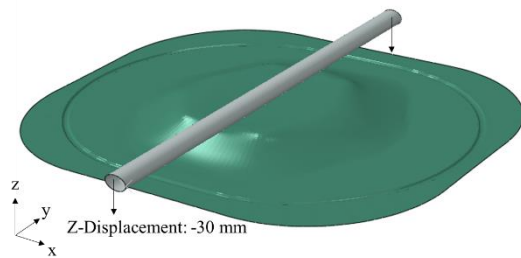
Figure 8. description of defined loading case
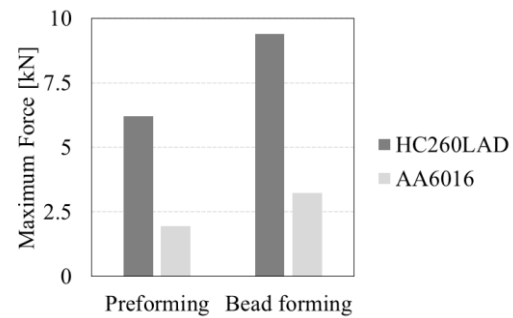
Figure 9. Stiffness effect by inserting bead geometries

4. Influence of process parameters on formability

Although the trajectories are used to provide the optimal bead path and geometry, it should be investigated whether the originally proposed bead design is actually producible. In other words, it is necessary to identify the influencing process parameters and the range of process parameter values which can produce the part, rather than which design brings the best effect. In order to investigate the reliability of producing the bead formed part, a probabilistic evaluation is desirable. LS-Opt optimization program [6] is used to perform the reliability analysis and the permissible process parameters space is identified.

4.1. Reliability analysis

Monte Carlo simulation is used for reliability analysis in LS-Opt program [6]. First, process variables affecting the part formability are selected. In this case, there are friction and blank holder force. The Monte Carlo simulation selects the random sample points according to the normal distribution, and the mean and standard deviation values of each parameter are shown in Table 1.

Table 1. Parameter range for the sampling

|	Blank holding force [kN]	Friction coefficient
Mean	1400	0.15
Standard deviation	100	0.05

Preforming and bead forming are carried out on the Abacus with the input parameter values from the sampling. Then, the major and minor strains of the formed part are imported into GFLC-Excel at each step. The GFLC value is calculated and treated as the response value for the Monte Carlo analysis. The constraints is set to 1.0, since the material failure occurs when the GFLC value reaches 1.0. The sampling number is set to LS-Opt default 16 for three process parameters and HC260LAD and default 10 for two process parameters and AA6016.
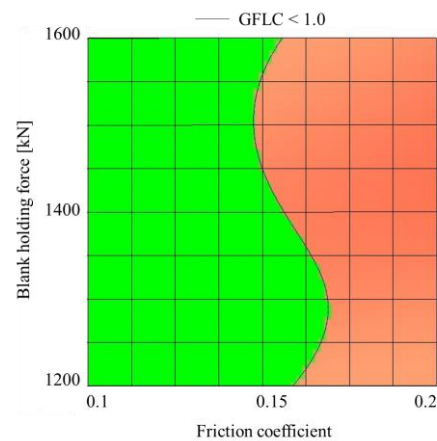
4.2. Feasibility

For HC260LAD, the correlation coefficient between the friction coefficient and the blank holding force is 0.08, and the correlation coefficient between the blank holding force and the GFLC value is -0.06. It can be seen that these relations do not have a large influence on each other. However, the

correlation coefficient between the friction coefficient and the GFLC value is -0.75, which indicates an inverse relationship. This can be bad for bead forming if the surface is too slippery. Figure 10 shows that the local instability appears at a friction coefficient of about 0.05. It is therefore necessary to avoid too much lubricating oil when the material HC260LAD and the bead tools against the load cases mentioned above are used.

For AA6016, the correlation coefficient between the friction coefficient and the blank holding force is 0.08 as for HC260LAD, and the correlation coefficient between the blank holding force and the GFLC value is -0.02, and these relations do not have a large influence on each other. It can be seen that it can be sufficiently manufactured within the defined blank holding force range. The correlation coefficient between the coefficient of friction and the GFLC is 0.87, which is highly correlated. That is, as the lubrication condition becomes worse, the aluminum formability is lowered and its influence is higher. As shown in Figure 11, the green color indicates the formable region, and the red indicates the non-formable region. At a value lower than the coefficient of friction of approximately 0.15, the product of AA6016 can be manufactured without material failure.
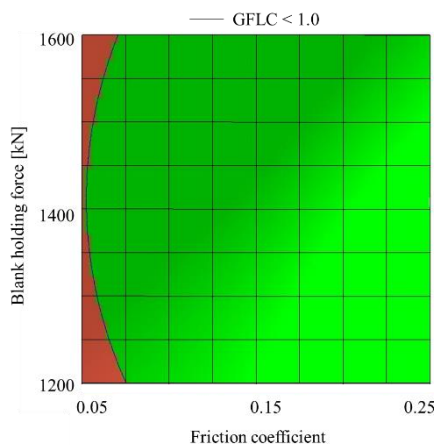
Figure 10. Feasibility area according to changes in process parameters for HC260LAD

Figure 11. Feasibility area according to changes in process parameters for AA6016
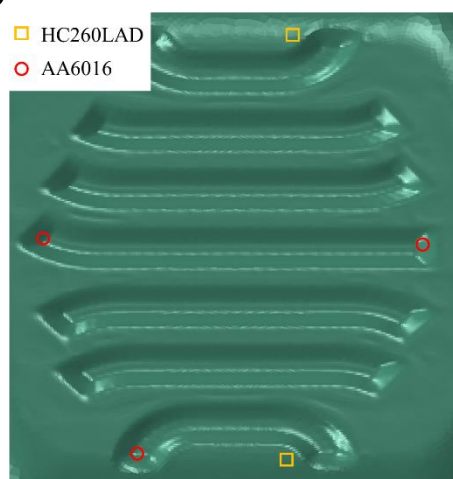
Figure 12. points where local instabilities occurred according to materials

Figure 12 shows where the local instabilities are predicted for each material. For material HC260LAD, the failure position points to hill of the bead geometry. This indicates that if the surface condition is too slippery, much material flows downward and the material thickness of the upper hill

becomes much thinner. On the contrary, for AA6016, the failure position indicates the bead wall side. If the lubrication is harsh, the material does not flow sufficiently inward, and the thickness of the material becomes much thinner on the wall.

By checking the location of material failure in the simulation, the result of the above reliability analysis was explained. The location or cause can be different even if the same failure value is shown. It was shown that the anisotropy characteristic of each material has an influence on the location of failure and the bead shape depending on the load case can be changed, so that the feasible range of process parameters, which can produce the part without the local instability, can be different. The validity of the material model was shown in the comparison of the directional tensile stress and r-value and the strain comparison of the modified Nakajima test, so that the results of the reliability analysis were indirectly validated. Later tools will be made and bead stamping experiments will be performed to directly ensure the accuracy of simulation and reliability analysis. Expected experimental reference values will be the strain position and the strain measurement.

5. Conclusion

In this study, non-AFR with Yld2000-2D was used to express the anisotropy of the exact sheet material. In order to determine the required material parameters, corresponding experiments were performed and the strain value, which is GFLC input value for formability determination, was calculated accurately after the experimental validation. It is obtained that the ideal bead path for maximizing the stiffness by using the OC-algorithm for a load case. This bead path was modified in consideration of the manufacturability and the stiffness of the part was increased by about 30 %. In order to know the range of process parameters that actually make this part possible, the reliability analysis was performed using LS-Opt. It is then necessary to increase the number of samples to obtain a more accurate results. Moreover, for the purpose of considering the possibility of the production of the optimization program, the reliability of the bead geometry will be analyzed as well as the process variables to investigate the feasible area of all variables that affect the producibility. As mentioned earlier, the direct validity of the model will be confirmed in future experiments.

References

[1]   Klein B 1995 in Technica, Rupperswil **44** 27-34
[2]   Clausen O N and Pedersen C B W 2009 *WCSMO-8 (Lisbon, Portugal)*
[3]   Albers A., Bursac N. and Rapp S, 2017 S. Forsch Ingenieurwes **81** 13-31
[4]   Volk V, Hoffmann H, Suh J and Kim J 2012 *CIRP Annals (Amsterdam, Holland)* **61** 259-62
[5]   Hill R, Proc. Roy. Soc. London, **193** 281-97
[6]   Barlat F, Brem J C, Yoon J W, Chung K, Dick R E, Lege D J, Pourboghrat F, Choi S –H and Chu E 2003 Int. J. Plasticity **19** 1297-1319
[7]   LS-OPT User's Manual 2015 Version 5.2
[8]   Abaqus 6.12 Documentation
[9]   Volk V and Suh J 2013 AIP Conference Proc. **1567** 556-61;
[10]   Yoon J.W., Stoughton T.B. and Dick R.E. 2007 AIP Conference Proc. **908** 685-690
[11]   Swift H.W. 1952 J. Mech. Phys. Solids **1** 1-18
[12]   Hockett J.E. and Sherby O.D. 1975 J. Mech. Phys. Solids **23** 87-98
[13]   Barlat F, Aretz H, Yoon J W, Karabin M E, Brem C J and Dick R E 2005 Int. J. Plasticity **21** 1009-39
[14]   Cha W-G, Vogel S, Bursac N, Albers A and Volk W 2016 J. Phys.: Conf. Ser. **734** 032077
[15]   Weinschenk A. and Volk W. 2017 *20th Int. ESAFORM Conf. on Material Forming* (Dublin: Dublin City University)